Confluence of Swallowtail Singularities of the Hyperbolic Schwarz Map Defined by the Hypergeometric Differential Equation

Masayuki Noro, Takeshi Sasaki, Kotaro Yamada, and Masaaki Yoshida

CONTENTS

2000 AMS Subject Classification: 33C05, 53C42

Keywords: Hypergeometric differential equation, hyperbolic Schwarz map, flat front, swallowtail singularity

The papers [Gálvez et al. 00, Kokubu et al. 03, Kokubu et al. 05] gave a method of constructing flat surfaces in three-dimensional hyperbolic space. Generically, such surfaces have singularities, since any closed nonsingular flat surface is isometric to a horosphere or a hyperbolic cylinder. In [Sasaki et al. 08a], we defined a map, called the hyperbolic Schwarz map, from one-dimensional projective space to three-dimensional hyperbolic space using solutions of the Gauss hypergeometric differential equation. Its image is a flat front and its generic singularities are cuspidal edges and swallowtail singularities. In this paper we study the curves consisting of cuspidal edges and the creation and elimination of swallowtail singularities depending on the parameters of the hypergeometric equation.

1. INTRODUCTION

We consider the Gauss hypergeometric differential equation

$$x(1-x)u'' + \{c-(a+b+1)x\}u' - abu = 0,$$

where (a, b, c) are complex parameters. By a change of the unknown u through multiplication by a nonzero function, we transform the equation into the SL form

$$u'' - q(x)u = 0,$$

where

$$q = -\frac{1}{4}\left(\frac{1-\mu_0^2}{x^2} + \frac{1-\mu_1^2}{(1-x)^2} + \frac{1+\mu_\infty^2-\mu_0^2-\mu_1^2}{x(1-x)}\right)$$
$$= -\frac{1}{4}\frac{(1-\mu_\infty^2)x^2 + (\mu_\infty^2+\mu_0^2-\mu_1^2-1)x + 1 - \mu_0^2}{x^2(1-x)^2},$$

and

$$\mu_0 = 1-c, \quad \mu_1 = c-a-b, \quad \mu_\infty = b-a.$$

1058-6458/2008 $0.50 per page
Experimental Mathematics **17**:2, page 191

For two linearly independent solutions u_0 and u_1 to this equation, we define the (multivalued) *hyperbolic Schwarz map*

$$HS : X = \mathbb{C} - \{0, 1\} \ni x \longmapsto U(x)\ {}^t\bar{U}(x) \in \mathbb{H}^3, \quad \text{(HS)}$$

where

$$U = \begin{pmatrix} u_0 & u_0' \\ u_1 & u_1' \end{pmatrix}.$$

The image lies in the three-dimensional hyperbolic space $\mathbb{H}^3$ identified with the space of positive 2×2 Hermitian matrices modulo diagonal ones.

We remark that the (multivalued) Schwarz map

$$S : X \ni x \longmapsto u_0(x) : u_1(x) \in \mathbb{P}^1 \quad \text{(S)}$$

and the (multivalued)derived Schwarz map

$$DS : X \ni x \longmapsto u_0'(x) : u_1'(x) \in \mathbb{P}^1 \quad \text{(DS)}$$

are regarded as maps with images in the ideal boundary of $\mathbb{H}^3$, which is identified with the complex projective line. The maps S and DS are connected by a one-parameter family of flat fronts in $\mathbb{H}^3$, and the map HS is one member of this family. We refer to [Gálvez et al. 00, Kokubu et al. 03, Sasaki et al. 08b] for these maps.

The image surface of X under HS is one of flat fronts studied in [Kokubu et al. 03]. The points 0 and 1 are singularities of the differential equation, and they may define ends generally. On the other hand, it is well known that generic singularities of fronts are cuspidal edges and swallowtails. In [Sasaki et al. 08a], we drew pictures of surfaces when the monodromy group of the equation is finite and when it is an elliptic modular group, paying attention especially to the curves of cuspidal edges and to the swallowtail singularities.

In this paper, we study the motion of such singularities depending on the parameters a, b, and c. Actually, we treat the case in which the parameters take special values: $a = \frac{1}{2}$, $b = \frac{1}{2}$, and $c = 1 - p$, where p is a real parameter. The reason we treat this case is that the hypergeometric differential equation admits a rich symmetry, so that computational arguments work fairly well. Moreover, when $p = 0$, we were able to draw nice pictures as in [Sasaki et al. 08a].

When p takes a general value, the number of points in the plane X where the map HS has swallowtail singularities is counted, and when p takes some special values, we encounter confluences of swallowtail singularities. Referring to the general theory of such confluences given in [Arnold 76, Langevin et al. 95], we study what happens in our case and show that two of the five types of confluences in [Langevin et al. 95] really occur, and one more type of confluence appears. From a computational point of view, we relied on the primary-decomposition algorithm of related ideals to obtain the special values of p and on computing the Sturm sequence associated with polynomials in order to count the number of swallowtail singularities.

2. SINGULARITIES OF THE IMAGE SURFACE

Relative to the differential equation in the SL form above, the conditions on the coefficient q so that the surface has cuspidal edges and swallowtails are given in the following lemma [Sasaki et al. 08a].

Lemma 2.1.

1. *A point $p \in X$ is a singular point of the hyperbolic Schwarz map HS if and only if $|q(p)| = 1$.*
2. *A singular point $x \in X$ of HS is equivalent to the cuspidal edge if and only if*
$$q'(x) \neq 0 \qquad \text{and} \qquad q^3(x)\bar{q}'(x) - q'(x) \neq 0.$$
3. *A singular point $x \in X$ of HS is equivalent to the swallowtail if and only if*
$$q'(x) \neq 0, \qquad q^3(x)\bar{q}'(x) - q'(x) = 0,$$
and
$$\Re\left\{\frac{1}{q}\left(\left(\frac{q'(x)}{q(x)}\right)' - \frac{1}{2}\left(\frac{q'(x)}{q(x)}\right)^2\right)\right\} \neq 0.$$

We apply the lemma to the hypergeometric equation. The set $\{|q| = 1\}$ is given as the curve

$$C = \{x : P_1(x, \bar{x}) = 0\},$$

where

$$P_1(x, \bar{x}) = |Q|^2 - 16|x^2(1-x)^2|^2$$

and

$$Q(x) = (1 - \mu_\infty^2)x^2 + (\mu_\infty^2 + \mu_0^2 - \mu_1^2 - 1)x + 1 - \mu_0^2.$$

The topological type of the curve C depends heavily on the number of real roots of the equation $P_1 = 0$. We next define R by

$$q' = -\frac{Q'x(1-x) - 2Q(1-2x)}{4x^3(1-x)^3} = \frac{-R(x)}{4x^3(1-x)^3},$$

S by

$$q^3(x)\bar{q}'(x) - q'(x) = \frac{S(x,\bar{x})}{4^4x^6(1-x)^6\bar{x}^3(1-\bar{x})^3},$$

and T by

$$\frac{1}{q}\left(\left(\frac{q'(x)}{q(x)}\right)' - \frac{1}{2}\left(\frac{q'(x)}{q(x)}\right)^2\right) = \frac{T(x,\bar{x})}{Q(x)Q(\bar{x})}.$$

We thus have three polynomials in x, $\bar{x}$, a, b, and c:

$$\begin{aligned}
R(x) &= x(1-x)Q' - 2(1-2x)Q,\\
S(x,\bar{x}) &= Q^3(x)R(\bar{x}) + 64x^3(1-x)^3\bar{x}^3(1-\bar{x})^3R(x),\\
T(x,\bar{x}) &= x(1-x)Q(\bar{x})(-16Q^2 - 8(1-2x)QQ'\\
&\quad + 6x(1-x)Q'^2 - 4x(1-x)QQ'').
\end{aligned}$$

We set

$$P_2 = \Re(S), \quad P_3 = \Im(S),$$

and

$$R_1 = \Re(R), \quad R_2 = \Im(R), \quad R_3 = \Re(T).$$

Then the singularity is a cuspidal edge if and only if

$$P_1 = 0, \quad \{P_2 \neq 0 \text{ or } P_3 \neq 0\}, \quad \{R_1 \neq 0 \text{ or } R_2 \neq 0\}$$

and is a swallowtail if and only if

$$\begin{aligned}
P_1 = 0, \quad P_2 = 0, \quad P_3 = 0,\\
\{R_1 \neq 0 \text{ or } R_2 \neq 0\}, \quad R_3 \neq 0.
\end{aligned}$$

2.1 Shape of the Curve C

We restrict our attention to the case $(a,b,c) = \left(\frac{1}{2},\frac{1}{2},c\right)$, and set $x = \left(\frac{1}{2}+s\right) + it$ and $c = 1-p$, where p is real. The polynomials P_i and R_i are polynomials in p, s, and t. They are symmetric relative to the reflections $s \leftrightarrow -s$, $t \leftrightarrow -t$, and $p \leftrightarrow -p$. Hence, we pay attention only to the case $p \geq 0$ in the following. Since $x = 0, 1$ are singularities of the coefficient q, the points $(s,t) = \left(\pm\frac{1}{2}, 0\right)$ are out of consideration.

Since $Q = 2c - c^2 - x + x^2$, P_1 is a polynomial of total degree 8 given as follows:

$$\begin{aligned}
P_1 = \frac{1}{2} + \frac{5}{2}s^2 - 2p^2s^2 + 16t^2s^4 - 16t^4s^2 - 64t^2s^6\\
- 96t^4s^4 - 64t^6s^2 + 6t^2s^2 + 2t^2p^2 - \frac{3}{2}p^2 - 16t^6\\
- 16t^8 - 5t^4 - \frac{5}{2}t^2 - 5s^4 + 16s^6 - 16s^8 + p^4.
\end{aligned}$$

The curve $\{(s,t) : P_1(p,s,t) = 0\}$ relative to the real coordinates (s,t) is denoted also by C. It depends on the value p and changes its shape as in Figures 1–3, where the value of the constants p_i will be given in the next subsection.

2.2 Swallowtail Points

We study the set $Z := \{(p,s,t);\ P_1 = P_2 = P_3 = 0\}$ using the primary-decomposition algorithm (refer, say, to [Greuel and Pfister 02]) that finds a set of generators of every minimal associated prime of the ideal $I := \langle P_1, P_2, P_3\rangle$ in the ring $\mathbb{Q}[p,s,t]$. The result is the following.

Lemma 2.2. *The set Z is the union of the sets defined by the following ideals:*

$$\begin{aligned}
I_1 &:= \langle p-1, (2s-1)^2 + 4t^2\rangle,\\
I_2 &:= \langle p-1, (2s+1)^2 + 4t^2\rangle,\\
I_3 &:= \langle p+1, (2s-1)^2 + 4t^2\rangle,\\
I_4 &:= \langle p+1, (2s+1)^2 + 4t^2\rangle,\\
I_5 &:= \langle t, 4s^4 - s^2 - p^2 + 1\rangle,\\
I_6 &:= \langle s, 8t^4 + 6t^2 + 2p^2 - 1\rangle,\\
I_7 &:= \langle H_0(p,t), H_1(p,s,t), H_2(p,s,t), H_3(p,s,t)\rangle,
\end{aligned}$$

where $H_0(p,t)$, $H_1(p,s,t)$, $H_2(p,s,t)$, are defined in Table 1.

Although the result was obtained by a "black box" algorithm, it can be verified if we are allowed to use the method of finding a Gröbner basis. Let G be a Gröbner basis of an ideal J with respect to a term order. We denote by $\mathrm{NF}_G(f)$ the remainder on dividing a polynomial f by G . Then $f \in J$ if and only if $\mathrm{NF}_G(f) = 0$; in this way, we can verify an ideal inclusion.

Lemma 2.2 is proved as follows. We first see that $I \subset I_i$, which implies that the locus $V(I_i)$ defined by the ideal I_i is a subset of Z. The converse inclusion $Z \subset \bigcup_{i=1}^7 V(I_i)$ follows from $\bigcup_{i=1}^7 V(I_i) = V(I_1I_2\cdots I_7)$ and $I_1I_2\cdots I_7 \subset \sqrt{I}$. In fact, $I_1I_2\cdots I_7$ is generated by $P := \{g_1g_2\cdots g_7 : g_i \in I_i (i = 1,\ldots,7)\}$, and we can verify $g^2 \in I$ for each $g \in P$ using a Gröbner basis of I.

Lemma 2.2 implies that the set Z consists of

$$\begin{aligned}
Z_1 &:= \{(p,s,0) : 4s^4 - s^2 - p^2 + 1 = 0\},\\
Z_2 &:= \{(p,0,t) : 8t^4 + 6t^2 + 2p^2 - 1 = 0\},\\
Z_3 &:= \{(p,s,t) : H_0(p,t) = H_1(p,s,t) = H_2(p,s,t)\\
&\qquad = H_3(p,s,t) = 0\}.
\end{aligned}$$

Note that the set defined by the ideal I_i, $1 \leq i \leq 4$, in Lemma 2.2 is included in Z_1. Figure 4 shows the set Z_1 projected to the space (s,p). The explicit representation is

$$s^2 = \left(1 \pm \sqrt{16p^2 - 15}\right)/8, \quad p = \pm\sqrt{4s^4 - s^2 + 1}.$$

The right-hand figure enlarges the upper part of the left-hand figure.

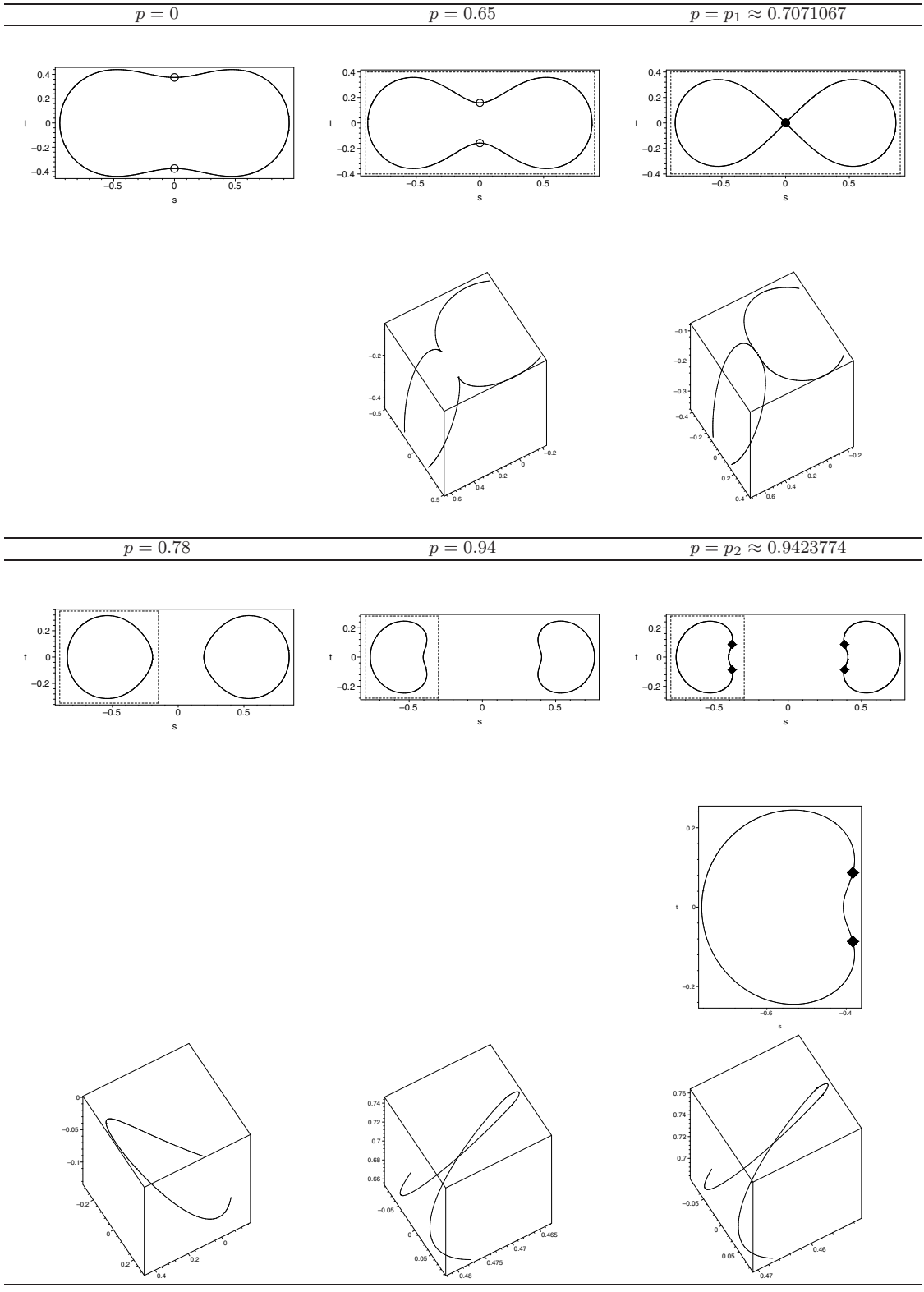

FIGURE 1. The curve C and the curve $\mathcal{C}$ (1).

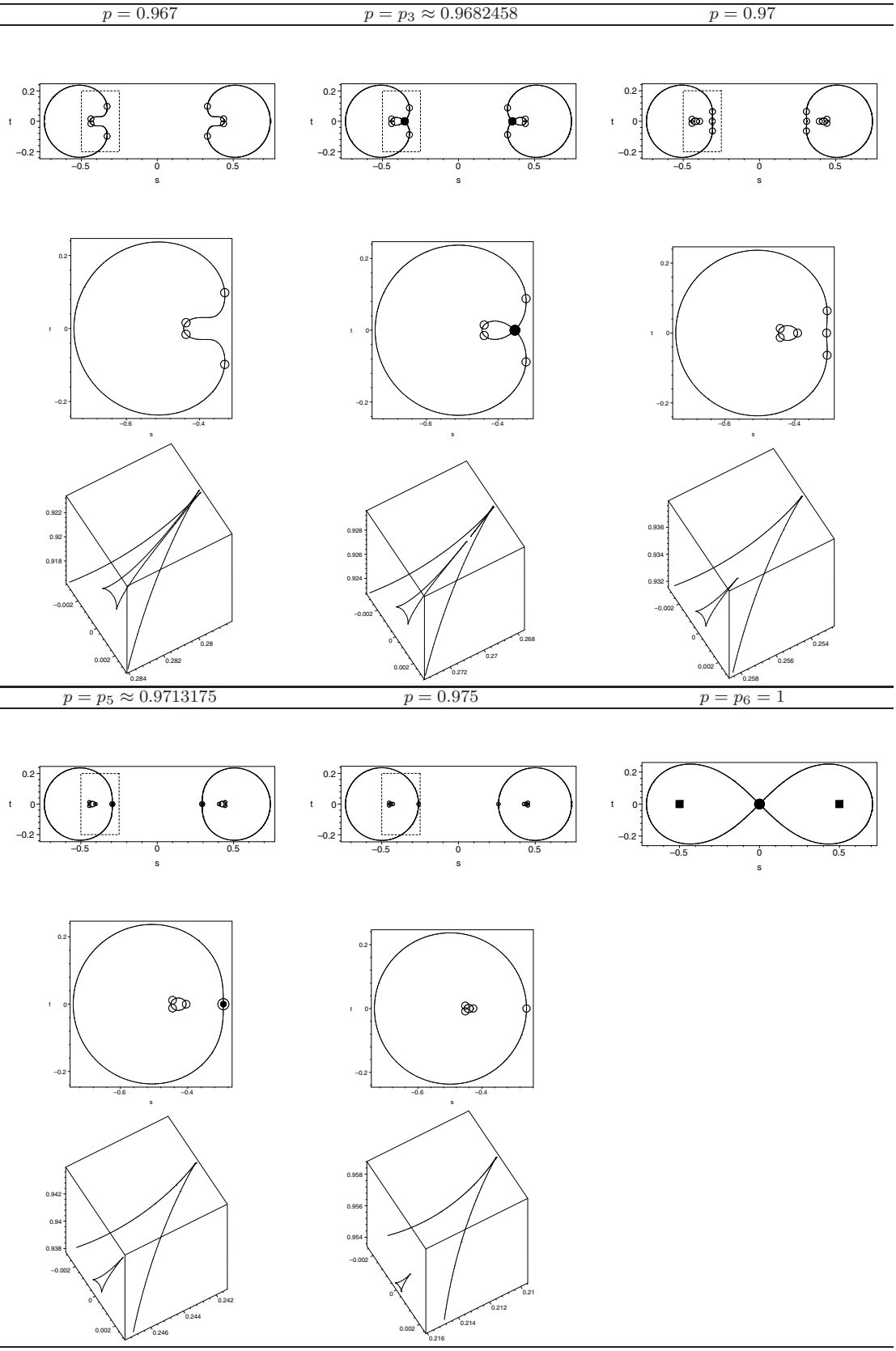

FIGURE 2. The curve C and the curve $\mathcal{C}$ (2).

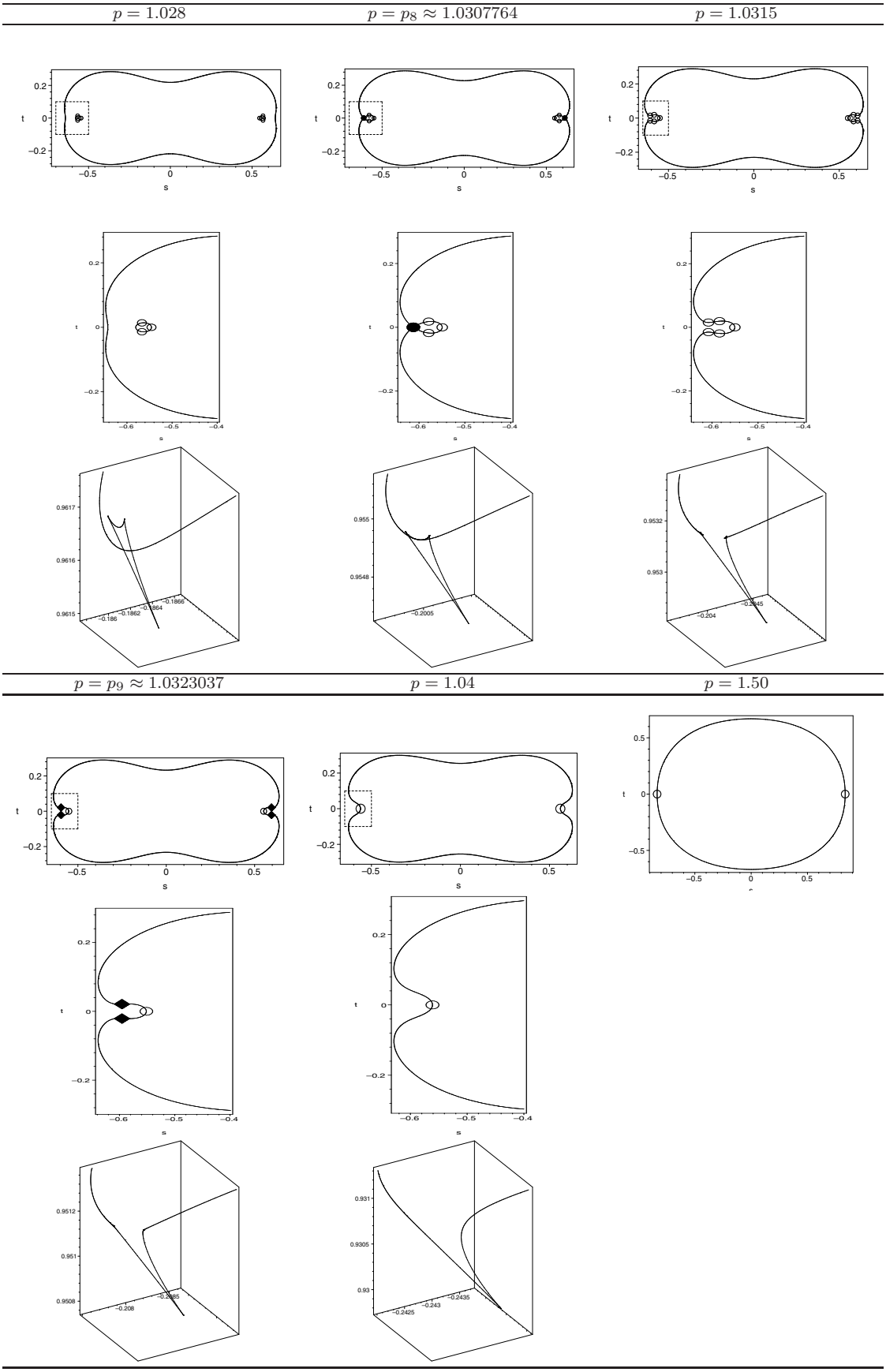

FIGURE 3. The curve C and the curve $\mathcal{C}$ (3).

$$
\begin{aligned}
H_0 &= (262144p^8 - 524288p^6 + 262144p^4)t^8 + (524288p^{10} - 1572864p^8 + 1687552p^6 - 735232p^4 + 79872p^2 + 16384)t^6 + (393216p^{12} - 1654784p^{10} \\
&\quad + 2817024p^8 - 2459136p^6 + 1142464p^4 - 260480p^2 + 21700)t^4 + (131072p^{14} - 737280p^{12} + 1755392p^{10} - 2289728p^8 + 1761920p^6 - 794968p^4 \\
&\quad + 192308p^2 - 18715)t^2 + 16384p^{16} - 118784p^{14} + 376000p^{12} - 679104p^{10} + 766068p^8 - 553296p^6 + 250232p^4 - 64912p^2 + 7412, \\
H_1 &= (-8192000p^{18} + 71680000p^{16} - 267673600p^{14} + 565094400p^{12} - 749209600p^{10} + 651990400p^8 - 375410912p^6 + 138995680p^4 - 30234388p^2 \\
&\quad + 2960012)s^2 + (-83886080p^{16} + 461373440p^{14} - 1033895936p^{12} + 1196949504p^{10} - 740818944p^8 + 222822400p^6 - 22544384p^4)t^6 \\
&\quad + (-125829120p^{18} + 786432000p^{16} - 2102657024p^{14} + 3123380224p^{12} - 2789900288p^{10} + 1502928896p^8 - 452747264p^6 + 55562240p^4 \\
&\quad + 4239360p^2 - 1409024)t^4 + (-62914560p^{20} + 458424320p^{18} - 1490173952p^{16} + 2838306816p^{14} - 3490809856p^{12} + 2877347840p^{10} \\
&\quad - 1598347904p^8 + 588634656p^6 - 138705184p^4 + 19590612p^2 - 1352780)t^2 - 10485760p^{22} + 94371840p^{20} - 391053312p^{18} + 980131840p^{16} \\
&\quad - 1640966144p^{14} + 1914822656p^{12} - 1580043904p^{10} + 917850432p^8 - 366915360p^6 + 96240468p^4 - 15040195p^2 + 1087441, \\
H_2 &= (-172748519424t^2 + 342090457088000p^{16} - 2647506597888000p^{14} + 8502392953446400p^{12} - 15007782165760000p^{10} + 16125961477836800p^8 \\
&\quad - 10936659362160000p^6 + 4626862256233568p^4 - 1127440491359040p^2 + 122038029361684)s^2 + (3503006280581120p^{14} \\
&\quad - 15725697150484480p^{12} + 27286047559778304p^{10} - 22422671555297280p^8 + 8286510388346880p^6 - 927195522924544p^4)t^6 \\
&\quad + (5254509420871680p^{16} - 27529427791380480p^{14} + 59988842462314496p^{12} - 69830531227779072p^{10} + 45967246621245440p^8 \\
&\quad - 16318586888937472p^6 + 2406740047872000p^4 + 118811578937344p^2 - 58122468702208)t^4 + (2627254710435840p^{18} - 16487753934110720p^{16} \\
&\quad + 45567759200370688p^{14} - 72489552047398912p^{12} + 72546907718641664p^{10} - 46869348690018304p^8 + 19388801939481216p^6 \\
&\quad - 4981168098598560p^4 + 752756242889920p^2 - 55743159881812)t^2 + 437875785072640p^{20} - 3498277391564800p^{18} + 12794850594193408p^{16} \\
&\quad - 28001940223336448p^{14} + 40236544719603712p^{12} - 39314960801359872p^{10} + 26264510377602688p^8 - 11791213573216192p^6 \\
&\quad + 3403925190427360p^4 - 576100608409972p^2 + 44796791787623, \\
H_3 &= -43273504115712s^4 + (-174591366701056000p^{16} + 135459740713574400p^{14} - 436107021782650880p^{12} + 771439681502274560p^{10} \\
&\quad - 830362744371128320p^8 + 563958281567654592p^6 - 238888696995057865 6p^4 + 582795932673655872p^2 - 63153571220692772)s^2 \\
&\quad + (-178781559501881344 0p^{14} + 806067676525887488 0p^{12} - 1403531594578054388 8p^{10} + 1156443904072954675 2p^8 - 4282247261844406272p^6 \\
&\quad + 480262996655341568p^4)t^6 + (-268172339252822016 0p^{16} + 141023076922844774 40p^{14} - 308196007463912734 72p^{12} \\
&\quad + 359568590921286942 72p^{10} - 237118745894237962 24p^8 + 843117880489619456 0p^6 - 124605894478356480 0p^4 - 60931259457007616p^2 \\
&\quad + 30059710795074560)t^4 + (-134086169626411008 0p^{18} + 844090112508264448 0p^{16} - 233849665574431784 96p^{14} + 372734299412738785 28p^{12} \\
&\quad - 373629987206655201 28p^{10} + 241708423854106050 56p^8 - 100099736190711901 44p^6 + 257420627493231388 8p^4 - 389407674475545536p^2 \\
&\quad + 28850050377704036)t^2 - 223476949377351680p^{20} + 178975391847809024 0p^{18} - 655896938227505561 6p^{16} + 143790920331554406 40p^{14} \\
&\quad - 206931071213083627 52p^{12} + 202466240228421488 64p^{10} - 135420788927371838 72p^8 + 608610658722778592 0p^6 - 175872249945733232 0p^4 \\
&\quad + 297968123692665860p^2 - 23197985921481043
\end{aligned}
$$

TABLE 1. The polynomials $H_0(p,t)$, $H_1(p,s,t)$, $H_2(p,s,t)$, from Lemma 2.2.

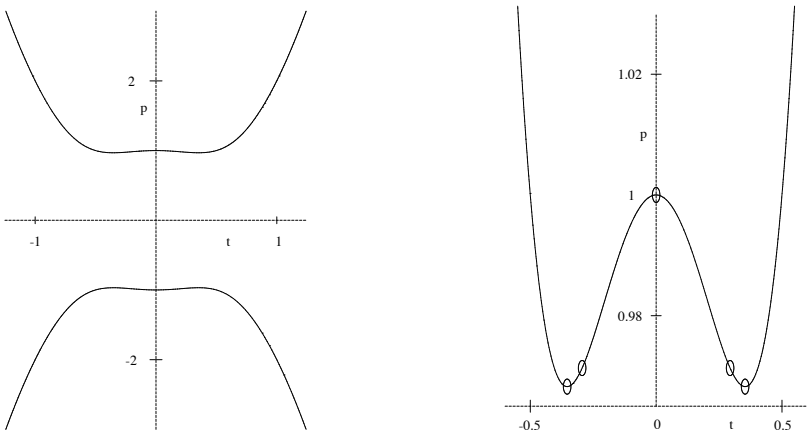

FIGURE 4. The set Z_1 projected to the space (s,p).

As we shall see in the next subsection, the circles in the right-hand figure denote those points that are worse than a swallowtail singularity: the p-coordinate of the top one is 1, that of middle ones is p_5, and that of the bottom ones is p_3, where

$$p_3 := \sqrt{15}/4 \approx 0.9682458365,$$
$$p_5 \approx 0.9713175204.$$

Thus, for any value of $p \in (p_3, 1)$, $p \neq p_5$, we have four swallowtail points, and for any value $p > 1$, two swallowtail points, both on the axis $t = 0$.

For the set Z_2 to have real points, it is necessary and sufficient that $-p_1 \leq p \leq p_1$, where

$$p_1 := 1/\sqrt{2} \approx 0.7071067810.$$

The explicit relation is

$$t^2 = \left(-3 + \sqrt{17 - 16p^2}\right)/8, \quad p = \pm\sqrt{1/2 - 3t^2 - 4t^4}.$$

For each value $p \in [0, p_1)$ we have two swallowtail points lying on the line $\{s = 0\}$. In the case $p = p_1$, the point $(s, t) = (0, 0)$ is not a swallowtail.

Summarizing the argument above, the number of swallowtail points belonging to $Z_1 \cup Z_2$ is given as follows:

p	0	$*$	p_1	$*$	p_3	$*$	p_5	$*$	1	$*$
Z_1	0	0	0	0	0	4	2	4	0	2
Z_2	2	2	0	0	0	0	0	0	0	0

Here $*$ stands for any value between the values of the two sides.

To study the set Z_3, we first deal with the polynomials H_2 and H_3. We can write

$$H_1(p, s, t) = c_1(p)s^2 + c_0(p, t),$$

where

$$\begin{aligned} c_1 = {} & -8192000p^{18} + 71680000p^{16} - 267673600p^{14} \\ & + 565094400p^{12} - 749209600p^{10} + 651990400p^8 \\ & - 375410912p^6 + 138995680p^4 - 30234388p^2 \\ & + 2960012. \end{aligned}$$

Then we can see first of all that $c_1 H_2$ and $(c_1)^2 H_3$ belong to the ideal $\langle H_0, H_1 \rangle$, which is verified by showing that $c_1 H_2 \bmod H_0$ and $(c_1)^2 H_3 \bmod H_0$ are divisible by H_1.

Hence, for each value for which $c_1(p) \neq 0$, the set Z_3 is the same as the set $\{H_0 = H_1 = 0\}$. Moreover, we can see that c_0^2 belongs to the ideal $\langle c_1, H_0 \rangle$ because c_1 divides the remainder $c_0^2 \bmod H_0$ with respect to t.

Hence, the set

$$\{(p, s, t) : p \geq 0, c_1 = H_0 = H_1 = 0\}$$

consists of lines in (p, s, t) space defined by $c_1(p) = H_0(p, t) = 0$, which are given as

$$\begin{aligned} (p, t) = {} & (p_4, \pm 0.011811323560992964937), \\ & (p_7, \pm 0.000192205787502698965), \\ & (p_{10}, \pm 0.022606558445778182272), \end{aligned}$$

where

$$p_4 \approx 0.97127920368420120746,$$
$$p_7 \approx 1.00370488167353310415,$$
$$p_{10} \approx 1.03276891081183183482.$$

The set

$$\{(p, s, t) : p \geq 0, c_1 = H_0 = H_1 = H_2 = H_3 = 0\}$$

consists of the points

$$\begin{aligned} (p, s, t) = {} & (p_4, \pm 0.4448235948, \pm 0.01181132356), \\ & (p_4, \pm 0.2944179698, \pm 0.01181132356), \\ & (p_7, \pm 0.5074847467, \pm 0.00019220578). \end{aligned}$$

Taking care of these exceptions, it is enough to study the set $\{(p, s, t) : H_0 = H_1 = 0\}$.

We next deal with the curve $H_0(t, p) = 0$ in the tp plane, where $p \geq 0$. Look at Figure 5. In order to know the precise shape of the curve, we use the Sturm sequence $\{f_0, f_1, \ldots, f_l\}$, which for a polynomial $f(t)$, is defined by the following recurrence:

$$\begin{aligned} & f_0 = f, \quad f_1 = \frac{df}{dt}, \\ & f_i = -(f_{i-2} \bmod f_{i-1}),\ i = 2, \ldots, l, \\ & f_{l-1} \bmod f_l = 0, \end{aligned} \tag{2–1}$$

where $(f_i \bmod f_{i-1})$ is the polynomial remainder. We define $\sigma(a)$ to be the number of sign changes in the sequence $\{f_0(a), f_1(a), \ldots, f_l(a)\}$, where zeros are not counted.

Theorem 2.3. (Sturm) [Jacobson 75]. *For $a, b \in \mathbb{R}$ such that $a < b$ and $f(a)$, $f(b) \neq 0$, the number of roots of $f(t)$ in the interval (a, b) is $\sigma(a) - \sigma(b)$. In particular, the number of all real roots of $f(x)$ is determined by the signs of the leading coefficients and the degrees of the f_i.*

Let $\ell = \{f_0(t), \ldots, f_l(t)\}$ ($f_i \in \mathbb{Q}(p)[t]$) be a sequence of polynomials obtained by applying the recurrence (2–1)

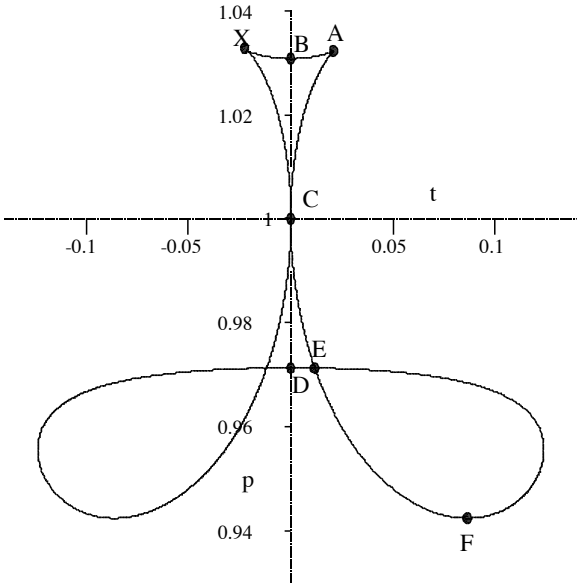

FIGURE 5. The curve $H_0(t,p)=0$.

to $f_0 = H_0$ with respect to t. Let $M \subset \mathbb{R}$ be the zeros of the numerators and denominators of the leading coefficients of the f_i, and so $\mathbb{R} \setminus M$ is the disjoint union of open intervals I_k. Then the sequence ℓ gives the correct Sturm sequence at each $p \in \mathbb{R} \setminus M$, and Theorem 2.3 ensures that the number of roots of H_0 is constant for all $p \in I_k$. It is clear that each branch $t = t(p)$ such that $H_0(p, t(p)) = 0$ over I_k is a continuous function of p. If $p \in M$, then p is a root of an irreducible polynomial over $\mathbb{Q}$ and we can compute the Sturm sequence over an algebraic number field $\mathbb{Q}(p)$. The Sturm sequence at each p tells the number of roots $t(p)$ within any interval, and we can draw the curve with desired precision.

The set M contains the zeros of the discriminant of the equation $H_0 = 0$, and we get the coordinates (p,t) of several extreme points as in the figure:

$$X = (p_{10}, 0.02260655844), \quad A = (p_9, 0.02095131175),$$
$$B = (p_8, 0), \quad C = (p_6, 0), \quad D = (p_5, 0),$$
$$E = (p_4, 0.01181132356), \quad F = (p_2, 0.08654627008),$$

where

$$p_2 \approx 0.94237741898935061,$$
$$p_6 = 1,$$
$$p_8 \approx 1.03077640441513745,$$
$$p_9 \approx 1.03230371163023017.$$

(Since the point X is very near to A, the point $(p_{10}, -0.0226065584)$ instead is drawn in the figure.)

For each point (p,t) on the curve $H_0(p,t) = 0$, we solve the equation $H_1(p,s,t) = 0$. Then, since $H_1(p,s,t) = c_1(p)s^2 + c_0(p,t)$, the number of real solutions depends on the signs of $c_1(p)$ and $c_0(p,t)$. To determine the sign of $c_0(p,t)/c_1(p)$, we enlarge the set M by adjoining the values of p satisfying $c_0 = H_0 = 0$ for some t, and the zeros of c_1, and then recompute I_k. Here note that the set $\{c_0 = H_0 = 0\}$ is discrete because the resultant of c_0 and H_0 with respect to the variable t turns out to be a nontrivial polynomial of p.

Let $t = t(p)$ be the continuous function over I_k discussed above. Then $c_0(p, t(p))/c_1(p)$ is also continuous, and its sign is constant over I_k because the numerator does not vanish over I_k. Thus we can determine the number of solutions by evaluating $c_0(p, t(p))/c_1(p)$ at a point $p \in I_k$. For $p \in M$, we have to deal with an algebraic number field again; we omit the details.

2.3 Nonswallowtail Points

If for some p, the point (s,t) is a swallowtail, then $(p,s,t) \in Z$. However, not all points in Z are swallowtails. We need to check the condition ($R_1 \neq 0$ or $R_2 \neq 0$) and the condition $R_3 \neq 0$, namely, the condition $q' \neq 0$ and the condition $\Re(T) \neq 0$, respectively. This check is done by studying the sets

$$E_1 := \{(p,s,t) : p \geq 0, P_1 = P_2 = P_3 = R_1 = R_2 = 0\}$$

and

$$E_2 := \{(p,s,t) : p \geq 0, P_1 = P_2 = P_3 = R_3 = 0\},$$

by relying on the primary decomposition of the corresponding ideals $\langle P_1, P_2, P_3, R_1, R_2\rangle$ and $\langle P_1, P_2, P_3, R_3\rangle$.

Lemma 2.4. *The set defined by the ideal $\langle P_1, P_2, P_3, R_1, R_2\rangle$ over the real field is the union of the sets defined by the ideals*

1. $\langle p-1, t, s\rangle$,
2. $\langle p-1, t, 2s-1\rangle$,
3. $\langle p-1, t, 2s+1\rangle$,
4. $\langle p-1, 4s-1, 16t^2+1\rangle$,
5. $\langle p-1, 4s+1, 16t^2+1\rangle$,
6. $\langle p-1, s, 4t^2+1\rangle$,
7. $\langle p+1, t, s\rangle$,
8. $\langle p+1, t, 2s-1\rangle$,

9. $\langle p+1, t, 2s+1\rangle$,
10. $\langle p+1, 4s-1, 16t^2+1\rangle$,
11. $\langle p+1, 4s+1, 16t^2+1\rangle$,
12. $\langle p+1, s, 4t^2+1\rangle$,
13. $\langle 2p^2-1, t, s\rangle$,
14. $\langle 16p^2-17, t, 8s^2-3\rangle$,
15. $\langle 16p^2-15, t, 8s^2-1\rangle$,
16. $\langle 16p^2-17, s, 8t^2+3\rangle$,
17. $\langle 16p^2-15, s, 8t^2+1\rangle$,
18. $\langle 20p^2-19, 80t^2+3, 80s^2-3\rangle$.

By this lemma we can see the following. The ideals numbered $4, 5, 6, 10, 11, 12, 16, 17, 18$, have no real points. The ideals $1, 2, 3, 7, 8, 9$, yield the three points

$$(1,0,0), \quad \left(1, \pm\frac{1}{2}, 0\right),$$

and the ideals $13, 14, 15$, yield the five points

$$(p_1, 0, 0), \quad (p_8, \pm s_1, 0), \quad (p_3, \pm s_2, 0),$$

in E_1(recall that we assumed $p \geq 0$), where

$$p_8 = \sqrt{17}/4 \approx 1.03077640, \quad s_1 = \sqrt{3/8} \approx 0.61237,$$
$$s_2 = 1/\sqrt{8} \approx 0.35355.$$

Lemma 2.5. *The set defined by the ideal $\langle P_1, P_2, P_3, R_3\rangle$ over the real field is the union of the sets defined by the ideals*

19. $\langle p-1, 4s^2-4s+4t^2+1\rangle$,
20. $\langle p-1, 4s^2+4s+4t^2+1\rangle$,
21. $\langle p+1, 4s^2-4s+4t^2+1\rangle$,
22. $\langle p+1, 4s^2+4s+4t^2+1\rangle$,
23. $\langle 4p^2-3, 4s-1, 16t^2+1\rangle$,
24. $\langle 4p^2-3, 4s+1, 16t^2+1\rangle$,
25. $\langle r_1(p), s, r_2(p,t)\rangle$,
26. $\langle r_3(p), t, r_4(p,s)\rangle$,
27. $\langle r_5(p), r_6(p,s), r_7(p,t)\rangle$,

where

$$\begin{aligned}
r_1(p) &= 256p^6 - 464p^4 + 224p^2 - 19,\\
r_2(p,t) &= 24t^2 + 64p^4 - 84p^2 + 29,\\
r_3(p) &= 256p^6 - 560p^4 + 416p^2 - 109,\\
r_4(p,s) &= 24s^2 - 64p^4 + 108p^2 - 47,\\
r_5(p) &= 262144p^{14} - 1458176p^{12} + 3352128p^{10}\\
&\quad - 4064896p^8 + 2723312p^6 - 934456p^4\\
&\quad + 111981p^2 + 7964,\\
r_6(p,s) &= 105137152s^2 + 805737070592p^{12}\\
&\quad - 3734052323328p^{10} + 6842337426624p^8\\
&\quad - 6160590983296p^6 + 2674420712784p^4\\
&\quad - 400807788840p^2 - 27034171281,\\
r_7(p,t) &= 105137152t^2 + 1275266859008p^{12}\\
&\quad - 6003856457728p^{10} + 11187800841024p^8\\
&\quad - 10256897785728p^6 + 4544374234288p^4\\
&\quad - 701552747480p^2 - 45094112399.
\end{aligned}$$

In this lemma, the cases $19, 20, 21, 22$, yield the two points

$$\left(1, \pm\frac{1}{2}, 0\right)$$

in E_2, and the cases $23, 24, 25$, yield no real points. For the ideal 26, by solving $r_3(p) = 0$, we get a real positive solution $p = p_5$. The corresponding values of s are determined by the equation $r_4(p,s) = 0$. We thus have the two points

$$(p_5, \pm 0.2939504177, 0)$$

in E_2. For the last ideal, 27, by solving $r_5(p) = 0$, we get real positive solutions $p = p_2$ and p_9. The corresponding values of (s,t) are determined by solving $r_6(p,s) = r_7(p,t) = 0$. The result is

$$(p_2, \pm 0.3834951026, \pm 0.08654627008),$$
$$(p_9, \pm 0.5955418899, \pm 0.02095131175).$$

Summarizing the argument above, the number of the swallowtail points belonging to Z_3 where $p \geq 0$ is given as follows:

p	p_2	$*$	p_5	$*$	$p_6 = 1$	$*$	p_8	$*$	p_9	$*$
Z_3	0	8	4	4	0	4	4	8	0	0

2.4 Numbers of Swallowtail Singularities

As we mentioned earlier, we restrict our consideration to the range of p in the interval $[0, \infty)$. Combining the

considerations in the previous two subsections, the exceptional values of p for which the point (p, s, t) in Z is not a swallowtail are

$$p_1,\ p_2,\ p_3,\ p_5,\ p_6 = 1,\ p_8,\ p_9. \tag{2–2}$$

We remark that the values p_4 and p_7 that appeared in the course of study of the set Z turn out not to be exceptional and that the exceptional values of p are classified into the three cases:

$$\begin{aligned} &q' = 0 \text{ and } \Re(T) \neq 0 : p_1, p_3, p_6 \text{ at } (0,0), p_8, \\ &q' \neq 0 \text{ and } \Re(T) = 0 : p_2, p_5, p_9, \\ &q' = 0 \text{ and } \Re(T) = 0 : p_6 \text{ at } \left(\pm\frac{1}{2}, 0\right). \end{aligned}$$

Now we sum up the above data and get the number N of swallowtail singularities:

p	0	$*$	p_1	$*$	p_2	$*$	p_3	$*$
N	2	2	0	0	0	8	8	12
p	p_5	$*$	$p_6 = 1$	$*$	p_8	$*$	p_9	$*$
N	6	8	0	6	6	10	2	2

In Figures 1–3, the swallowtail singularities are represented by circles; other symbols represent worse singularities, as explained in the next section.

Remark 2.6. The number N counts the swallowtail singularities in the plane $x = \frac{1}{2} + s + it$, not those on the image surface; recall that the hyperbolic Schwarz map *HS* is multivalued.

3. CONFLUENCE OF SWALLOWTAIL SINGULARITIES

In the previous section, we studied the variation in the number of swallowtail singularities as p runs from 0 to ∞. On the other hand, the confluence of swallowtail singularities has been studied by Arnold [Arnold 76]. Figure 6 is taken from [Langevin et al. 95, Figure 3], which shows five types $(1, \ldots, 5)$ of confluence (bifurcation) of swallowtail singularities. The types 1, 2, and 5 are called the pair of cuspidal lips, the pair of cuspidal beaks, and type A_4, respectively; see [Saji et al. 07].

From the study in the last section, we observe that types 2 and 5 actually occur in our move, and that another type of confluence also occurs. In Figures 1–3, they are indicated respectively by

$$\bullet \text{ (type 2)}, \quad \blacklozenge \text{ (type 5)}, \quad \odot.$$

In this section, the (local) image surface is denoted by $\mathcal{S}$, and the (local) image of the curve C under the hyperbolic Schwarz map *HS* is denoted by $\mathcal{C}(\subset \mathcal{S})$.

3.1 • Around $p = p_1$, $p = p_3$, $p = p_6$, and $p = p_8$

When $p < p_1$, there is a pair of swallowtail singularities on $\mathcal{S}$ carried by a pair of cuspidal components of $\mathcal{C}$. As p tends to p_1, two singularities come together and kiss, and when $p_1 < p$, then $\mathcal{C}$ becomes a pair of nonsingular curves. We observe that this move is of type 2 in Figure 6. See also Figure 7, which represents the image surface $\mathcal{S}$ under *HS* of the square $\{(s,t) : -0.5 < s < 0.5, -0.5 < t < 0.5\}$. Something similar happens when $p \searrow p_3$, $p \searrow p_8$, and $p \nearrow p_6$ around $(s,t) = (0,0)$.

3.2 ♦ Around $p = p_2$ and $p = p_9$

When $p \leq p_2$, there are no swallowtail singularities. However, when $p > p_2$, there are four pairs of swallowtail singularities, eight in all. The move around p_2 is observed to be of type 5 in Figure 6. Such a pair is drawn in Figure 8 (left) when $p = 0.945$. The lower picture is the curve $\mathcal{C}$, carrying two swallowtails, which reside at the two cusps of this curve. The upper picture is a tubular neighborhood in the surface $\mathcal{S}$ of the curve $\mathcal{C}$. Something similar happens when $p \searrow p_9$.

3.3 ⊙ Around $p = p_5$

As $p \nearrow p_5$, three swallowtail singularities shrink to one point that is not a swallowtail singularity, and after passing p_5, one swallowtail singularity reappears immediately. It is a move of type A_5; we refer to [Saji et al. 07] for its characterization. Note that this move is not among Arnold's five moves in Figure 6. Figure 8 (right) shows the curve $\mathcal{C}$ with three cusps and the surface $\mathcal{S}$ around this curve.

3.4 Around $p = p_6$

When $p = p_6 = 1$, there are no swallowtails. In Figure 2, ■ denotes the singularities $x = 0$ and $x = 1$ of the differential equation. If p moves away from 1, then three swallowtail singularities appear in both directions. In Figure 9, the left picture is the image of a small square situated to the right of the point $(s,t) = (-0.5, 0)$ (singular point of the differential equation) including three swallowtails when $p = 0.975$. They shrink to one point, the image of the point $x = 0$, as p tends to 1.

The right picture is the image of a small square situated to the left of the point $(-0.5, 0)$ including three swallowtails when $p = 1.028$. Though this move resembles the move of type 3 in Figure 6, it is different in that it occurs at the singular points of the differential equation, where the map is multivalued.

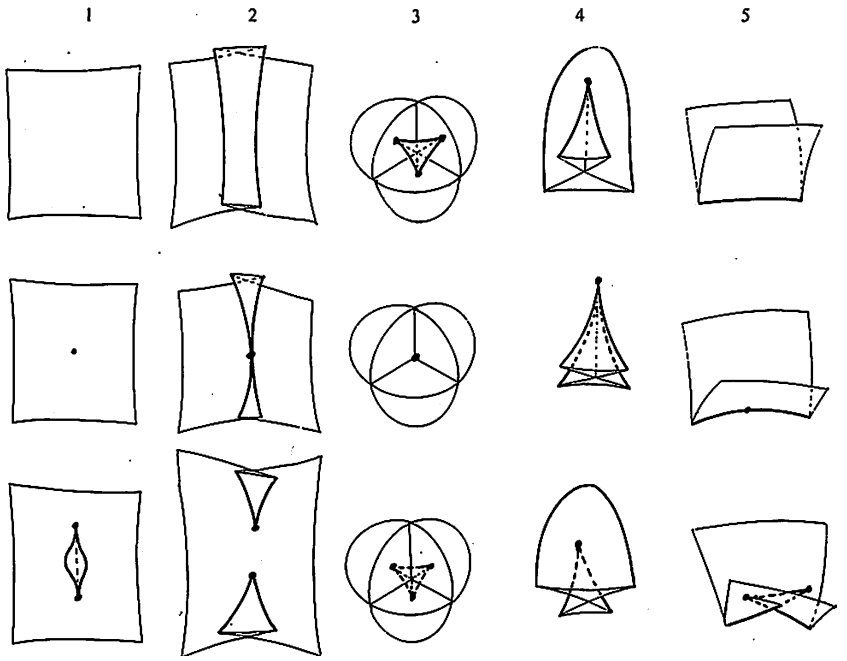

FIGURE 6. Confluence of swallowtail singularities from [Langevin et al. 95, Figure 3].

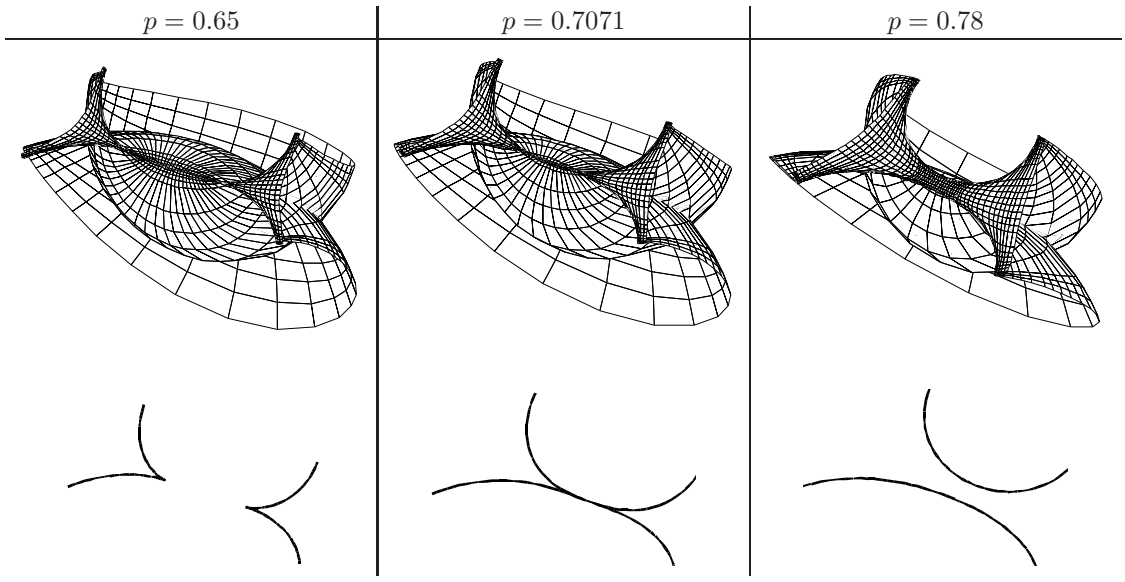

FIGURE 7. The images under *HS* (1): the images of the square $(-0.5, 0.5) \times (-0.5, 0.5)$ and the curve $\mathcal{C}$ in it.

3.5 Drawing Figures

We give here some additional information about the figures. Figures 1–3 show the curve C. Each first row gives a global view, and the second row for $p \geq 0.78$ gives a finer view of a part of C. The marks •, ⧫, ⊙, and ■ are drawn in a somewhat emphasized manner.

In the third row (second row when $p \leq p_1$), the image curves $\mathcal{C}$ are given; the range of the drawing is indicated by a dotted rectangle in the figures of the first rows.

$p = 0.945$	$p = 0.971$
	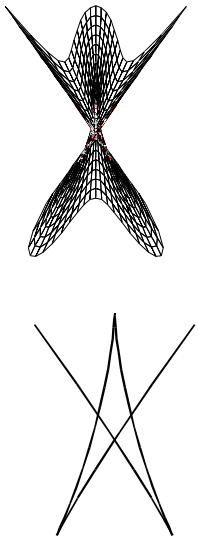
The images of the rectangle $(0.375, 0.395) \times (0.01, 0.135)$ and the curve C	The images of a narrow strip along the segment $s \approx 0.2975$, $t \in (-0.05, 0.05)$ and the curve C

FIGURE 8. The images under HS (2).

$p = 0.975$	$p = 1.028$
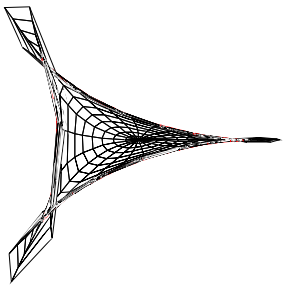	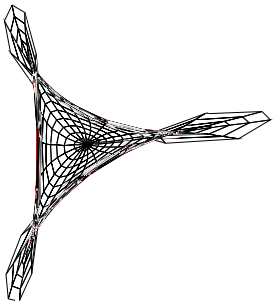
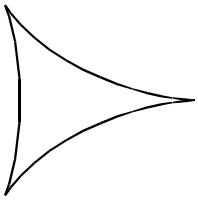	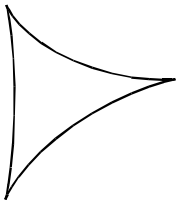
The images of the rectangle $(-0.46, -0.41) \times (-0.01, 0.01)$ and the curve C	The images of the rectangle $(-0.57, -0.54) \times (-0.01, 0.01)$ and the curve C

FIGURE 9. The images under HS (3).

When $p < 1$, the map HS defined in the upper half-plane is continued analytically through the interval $0 < x < 1$, and when $p > 1$, through the negative real axis $x < 0$.

Figure 7 shows the images $\mathcal{S}$ of the square $\{(s,t) : s \in (-0.5, 0.5), t \in (-0.5, 0.5)\}$, where the image curves $\mathcal{C}$ are drawn in greater detail than in Figure 1.

Figures 8 and 9 depict $\mathcal{S}$ and $\mathcal{C}$ for distinct values of p.

ACKNOWLEDGMENTS

The authors wish to express their thanks to the referees, who gave several suggestions that improved the presentation of this paper.

REFERENCES

[Arnold 76] V. I. Arnol'd. "Wave Front Evolution and Equivariant Morse Lemma." *Comm. Pure Appl. Math.* 29 (1976), 557–582.

[Gálvez et al. 00] J. A. Gálvez, A. Martínez, and F. Milán. "Flat Surfaces in Hyperbolic 3-Space." *Math. Annalen* 316 (2000), 419–435.

[Greuel and Pfister 02] G.-H. Greuel and G. Pfister. *A Singular Introduction to Commutative Algebra*. Berlin: Springer, 2002.

[Iwasaki et al. 91] K. Iwasaki, H. Kimura, S. Shimomura, and M. Yoshida. *From Gauss to Painlevé: A Modern Theory of Special Functions*. Wiesbaden: Vieweg, 1991.

[Jacobson 75] N. Jacobson. *Lectures in Abstract Algebra 3: Theory of Fields and Galois Theory*, Graduate Texts in Math. 32. New York: Springer, 1975.

[Kokubu et al. 03] M. Kokubu, M. Umehara, and K. Yamada. "An Elementary Proof of Small's Formula for Null Curves in $\mathrm{PSL}(2,\mathbb{C})$ and an Analogue for Legendreian Curves in $\mathrm{PSL}(2,\mathbb{C})$." *Osaka J. Math.* 40 (2003), 697–715.

[Kokubu et al. 05] M. Kokubu, W. Rossman, K. Saji, M. Umehara, and K. Yamada. "Singularities of Flat Fronts in Hyperbolic Space." *Pacific J. Math.* 221 (2005), 303–351.

[Langevin et al. 95] R. Langevin, G. Levitt, and H. Rosenberg. "Classes d'homotopie de surfaces avec rebroussements et queues d'aronde dans $\mathbb{R}^3$." *Can. J. Math.* 47 (1995), 544–572.

[Saji et al. 07] K. Saji, T. Sasaki, and M. Yoshida. "Hyperbolic Schwarz Map of the Confluent Hypergeometric Differential Equation." Preprint, 2007.

[Sasaki et al. 08a] T. Sasaki, K. Yamada, and M. Yoshida. "Hyperbolic Schwarz Map for the Hypergeometric Equation." To appear in *Experiment. Math.*, 2008

[Sasaki et al. 08b] T. Sasaki K. Yamada, and M. Yoshida. "Derived Schwarz Map of the Hypergeometric Differential Equation and a Parallel Family of Flat Fronts." To appear in *Intern. J. Math.*, 2008.

[Yoshida 97] M. Yoshida. *Hypergeometric Functions, My Love*. Wiesbaden, Vieweg, 1997.

Masayuki Noro, Department of Mathematics, Kobe University, Kobe 657-8501, Japan (noro@math.kobe-u.ac.jp)

Takeshi Sasaki, Department of Mathematics, Kobe University, Kobe 657-8501, Japan (sasaki@math.kobe-u.ac.jp)

Kotaro Yamada, Faculty of Mathematics, Kyushu University, Fukuoka 812-8581, Japan (kotaro@math.kyushu-u.ac.jp)

Masaaki Yoshida, Faculty of Mathematics, Kyushu University, Fukuoka 810-8560, Japan (myoshida@math.kyushu-u.ac.jp)

Received February 20, 2007; accepted February 14, 2008.